ERS-2 SAR CYCLIC REPORT

28TH SEPTEMBER 2009 - 2ND NOVEMBER 2009 (CYCLE 151)

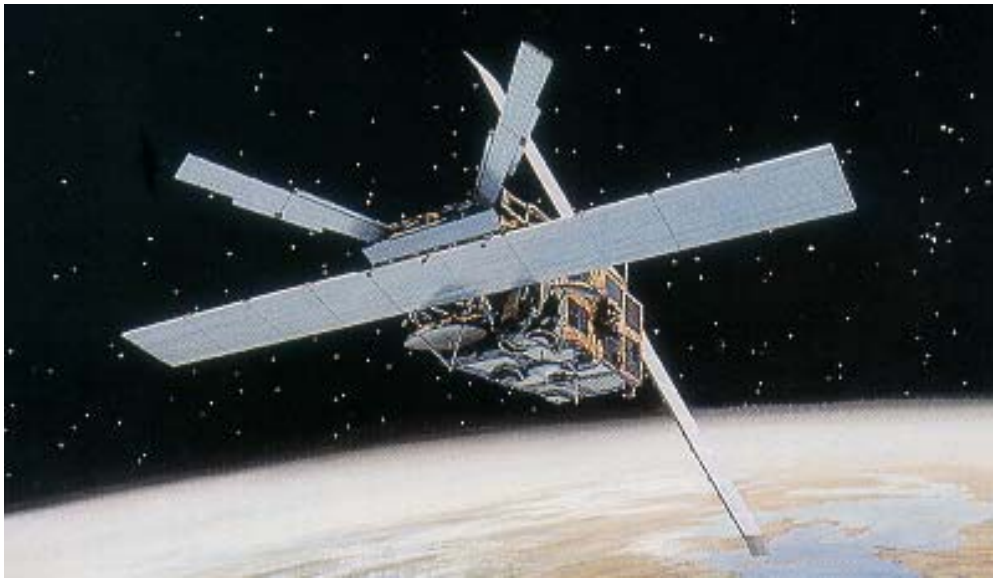

PUBLIC SUMMARY

prepared by/*préparé par*	IDEAS SAR Team
reference/*réference*	IDEAS-BAE-OQC-REP-0245
issue/*édition*	9
revision/*révision*	0
date of issue/*date d'édition*	13/11/2009
status/*état*	Approved
Document type/*type de document*	Technical Note
Distribution/*distribution*	

European Space Agency
Agence spatiale européenne

TABLE OF CONTENTS

1 EXECUTIVE SUMMARY

This document summarises the ERS-2 SAR instrument and product quality status as derived from data acquired up to and during repeat period cycle 151 from 28th September to 2nd November 2009. During this period there were no particular satellite or instrument problems.

The status of the instrument is provided in chapter 2 including details of any data disclaimers issued during the reporting period. Information on the internal calibration of both image and wave modes is presented in chapter 3. The radiometric stability of the ERS-2 SAR has been assessed via various approaches – transponders, the Amazon rainforest and ground stations, as described in chapter 4. Chapter 5 describes the important image quality parameter of noise equivalent radar cross-section. Details on the Doppler Centroid evolution are provided in chapter 6. Finally a list of auxiliary data files applicable to the ERS-2 SAR is provided in chapter 7.

A summary of the performance of the ERS-2 SAR can be found on the ESA Product Control Service web site at http://earth.esa.int/pcs/ers/sar/articles/.

2 INSTRUMENT STATUS

No particular satellite or instrument problems during the reporting period.

2.1 Instrument Unavailability

The following instrument unavailabilities occurred during the reporting period.

Unavailability report reference	Start	Stop	Additional Information
ER-UNA-2009/052	10 Oct 2009 07.42.26	10 Oct 2009 10.03.33	AMI switched to HEATER/REF due to COMMAND FAILURE
ER-UNA-2009/053	13 Oct 2009 12.40.44	13 Oct 2009 19.07.31	AMI Switchdown to Standby / MCMD INHIBIT Mode due to 222 FMT LEN

2.2 Data Disclaimer

No new data quality disclaimers were issued during the reporting period.

2.3 ERS-2 Mission Operations

Information about the operation of the ERS-2 mission can be found at: http://earth.esa.int/ers/technicalstatusreport/.

3 INTERNAL CALIBRATION

3.1 Image Mode Internal Calibration

The internal calibration of the ERS-2 SAR is assessed via calibration pulse, replica pulse and noise signal powers. The calibration pulse and noise signal are available at the start and end of each SAR imaging sequence while the replica pulses are available throughout an imaging sequence. The calibration pulse measures the majority of any gain drift from image sequence to image sequence while the replica pulse monitors any gain drift during the imaging sequence when the more representative calibration pulse is not available. In fact, the power of the calibration pulse is the best guide we have for the transmitted pulse power.

Figure 3.1 shows the calibration pulse power, replica pulse power and noise pulse power from the start of the ERS-2 mission. The calibration pulse power plot shows significant change of power during an image sequence, especially during recent years. ERS-2 SAR products generated within the ESA ground segment compensate for any variation in calibration pulse power during an imaging sequence (although there is an impact on the noise equivalent radar cross-section – see chapter 6). Note that the replica and noise pulse powers are only shown for the start of each imaging sequence.

Further details on the internal calibration on the ERS-2 SAR can be in the ERS-2 SAR performance paper available on the ESA Product Control Service web site (http://earth.esa.int/pcs/ers/sar/articles/).

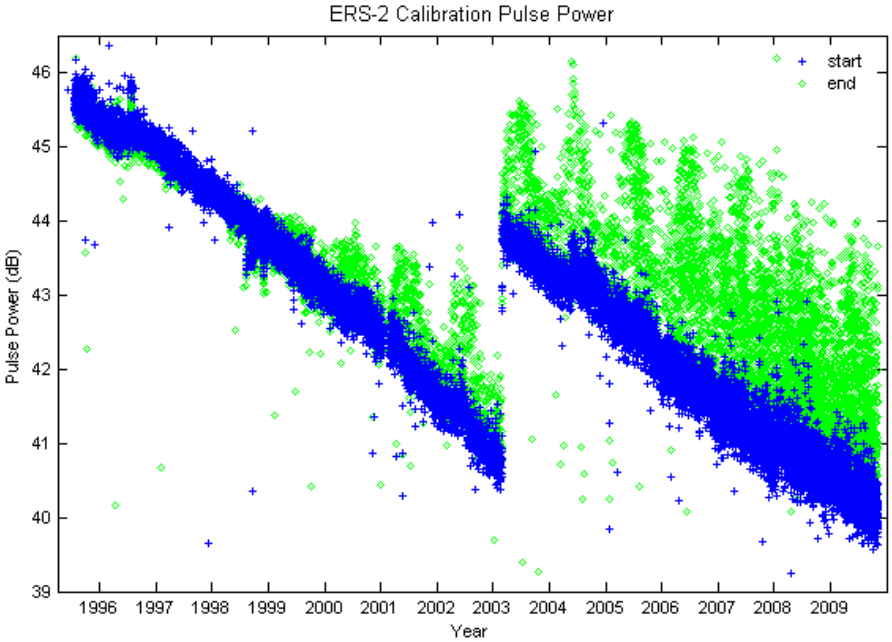

Figure 3.1(a). ERS-2 SAR Calibration Pulse Power

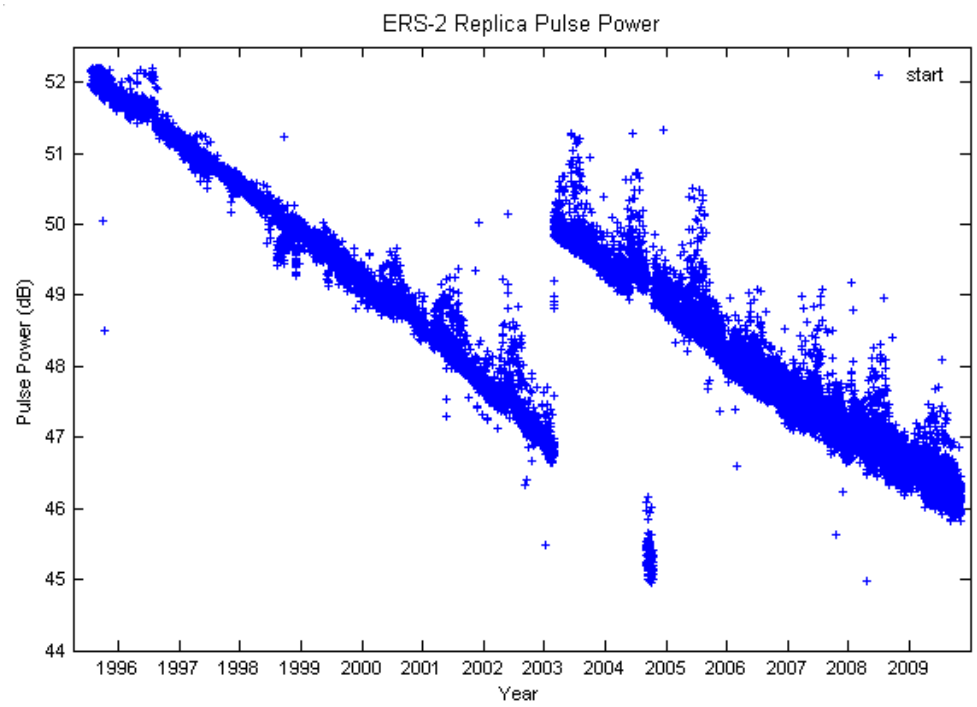

Figure 3.1(b). ERS-2 SAR Replica Pulse Power

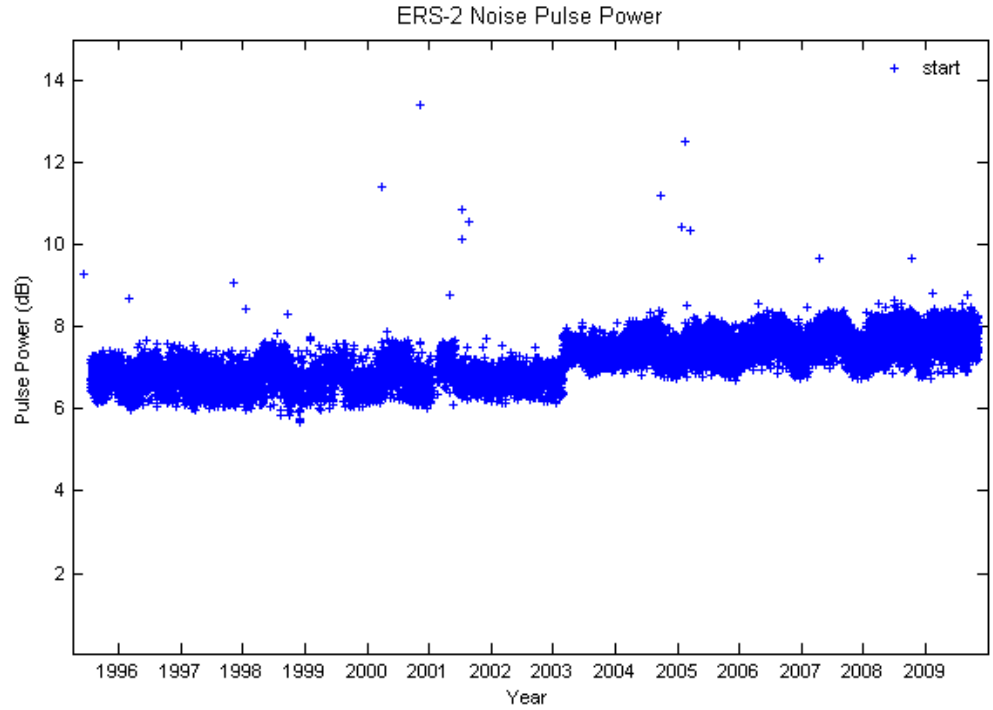

Figure 3.1(c). ERS-2 SAR Noise Pulse Power

3.2 Wave Mode Internal Calibration

As with image mode, a calibration pulse power is available for wave mode. Figure 3.2 (top) shows the daily averaged calibration pulse power since 1995 while Figure 3.2 (bottom) shows the calibration pulse power from each individual UWAND product since mid January 2009.

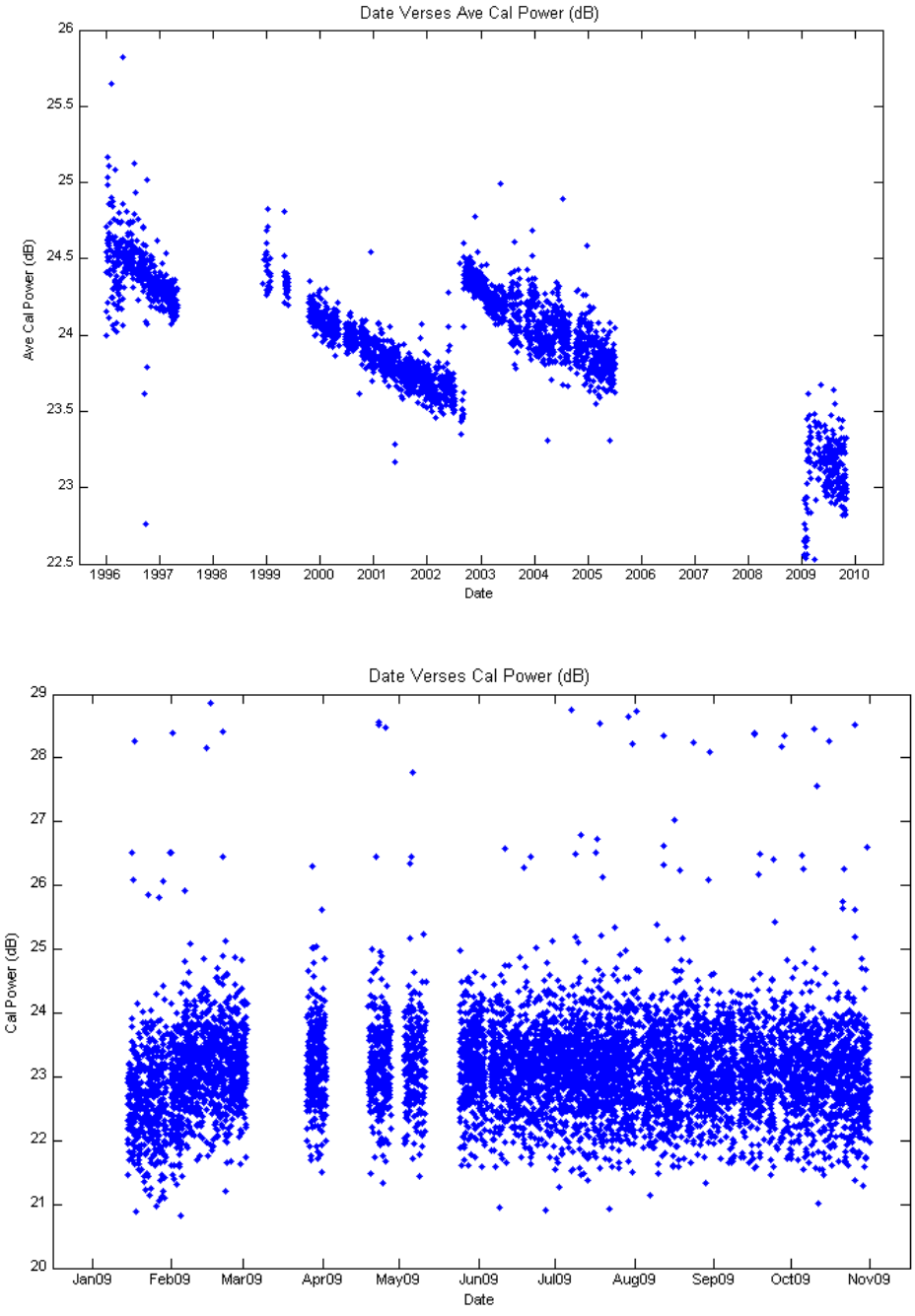

Figure 3.2 ERS-2 Wave Mode Calibration Pulse Power

4 IMAGE QUALITY

The quality of ERS-2 SAR imagery has been assessed via impulse response function (IRF) measurements using the three ESA transponders deployed in The Netherlands between April 1995 and November 2001. These measurements include the azimuth and range spatial resolutions, peak sidelobe ratio and integrated sidelobe ratio. Table 4.1 gives values for these parameters from the four look detected ground range IMP and single look complex slant range IMS products; as the IMP product range resolution varies across the swath, the table gives the range resolution converted to the mid-swath incidence angle of 23°. These IMP and IMS products have been processed with the PGS-ERS SAR processor deployed within the ESA ERS ground segment.

Table 4.1 shows that the measured azimuth and range resolutions compare well with theoretical values (20.98m for IMP azimuth resolution, 24.67m for IMP range resolution at 23° incidence angle, 4.87m for IMS azimuth resolution and 9.64m for IMS slant range resolution). The sidelobe ratios are all low and acceptable.

Parameter	IMP	IMS
Azimuth resolution	22.32±0.26m	5.42±0.02m
Range resolution	25.59±0.22m	9.96±0.11m
Integrated sidelobe ratio	-14.0±1.4dB	-15.1±0.7dB
Peak sidelobe ratio	-16.8±0.5dB	-21.8±0.7dB
Spurious sidelobe ratio	-23.6±1.5dB	-28.6±1.1dB

Table 4.1. ERS-2 SAR IMP and IMS image quality parameters

Corresponding IRF values for the previous ESA ERS ground segment SAR processor, the VMP, can be found in the ERS-2 SAR performance paper available on the ESA Product Control Service web site (http://earth.esa.int/pcs/ers/sar/articles/).

5 RADIOMETRIC STABILITY

The stability of the ERS-2 SAR has been measured using three ESA transponders (up to end 2001), the Amazon rainforest and ground receiving stations in Kiruna, Sweden and Neustrelitz, Germany.

Three ESA transponders were deployed across Flevoland, The Netherlands from the start of the ERS-2 mission in April 1995 until February 1997, April 2001 and November 2001 respectively. The measured radar cross-sections of the transponders were compared to their actual radar cross-section values. This relative transponder radar cross-section (after the power loss calibration correction has been applied) is shown in Figure 5.1. The measured mean radiometric accuracy, mean radiometric stability and peak to peak rcs for the ERS-2 SAR using the ESA transponders are shown in Tables 5.1 and 5.2. These tables indicate an excellent radiometric stability for the ERS-2 SAR. In addition, the radiometric accuracy value is very good while the peak to peak radar cross-section value is acceptable.

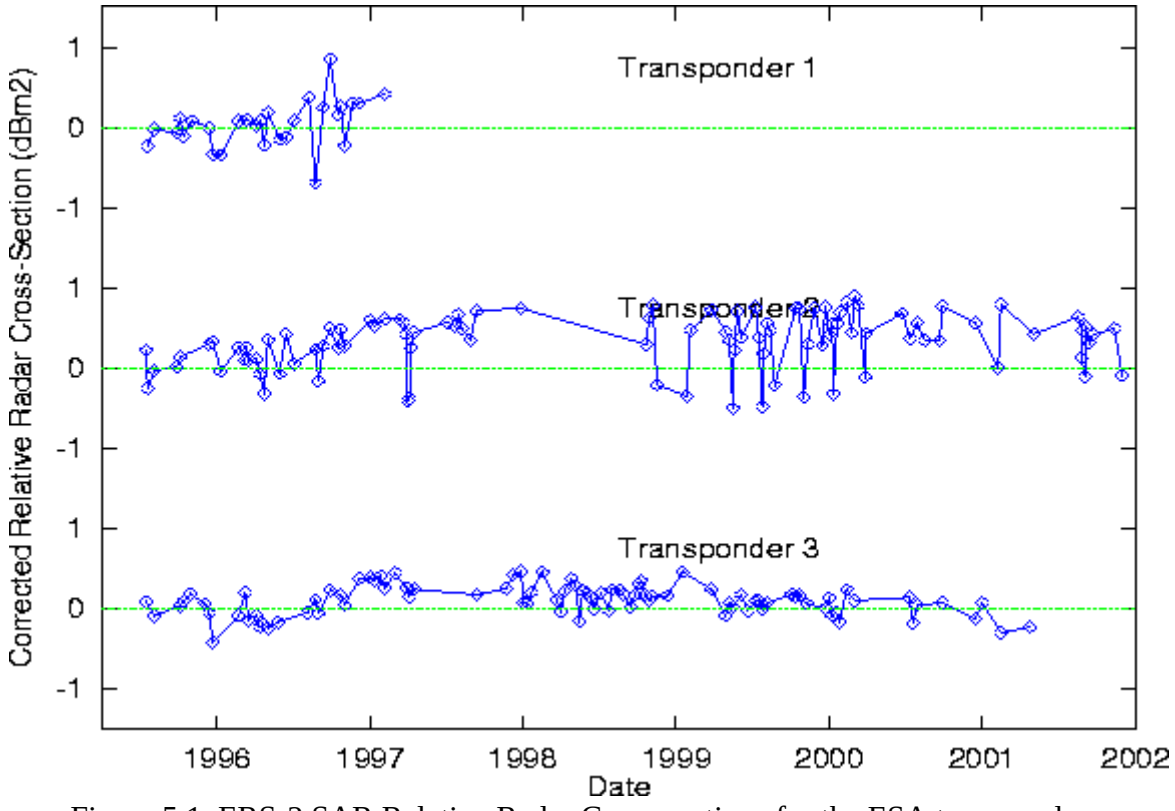

Figure 5.1. ERS-2 SAR Relative Radar Cross-sections for the ESA transponders.

Transponder	Operation Dates	Mean Accuracy (dB)	Mean Stability (dB)	Peak-Peak RCS (dB)	No of Images
ERS Tran. #1	19-Jul-95 – 05-Feb-97	0.04	0.29	1.54	28
ERS Tran. #2	19-Jul-95 – 30-Nov-01	0.33	0.34	1.39	100
ERS Tran. #3	19-Jul-95 – 25-Apr-01	0.11	0.18	0.88	92

Table 5.1. ERS-2 SAR Radiometric Results from ESA Transponders

Radiometric stability	0.27dB
Radiometric accuracy	0.16dB
Peak to peak radar cross-section	1.27dB

Table 5.2. Mean ERS-2 SAR radiometric results from the ESA transponders

ERS-2 SAR images of the Amazon rainforest have also been used to derive radiometric stability. The dataset is based on two nearby scene sites (track 139 and frame 3735 at centre latitude 6º 20'S, longitude 67º 13'W and track 146 and frame 7059 at centre latitude 6º 30'S, longitude 67º 33'W). Figure 5.2 shows gamma (= sigma0/cos(i) where sigma0 is radar cross-section and i is incidence angle) derived from each image after the masking of none rainforest areas. The mean gamma for the first site is -6.03dB while the stability is 0.15dB and for the second site the mean gamma is -5.94dB with a stability of 0.22dB. These stability values are comparable to the values derived using the ESA transponders.

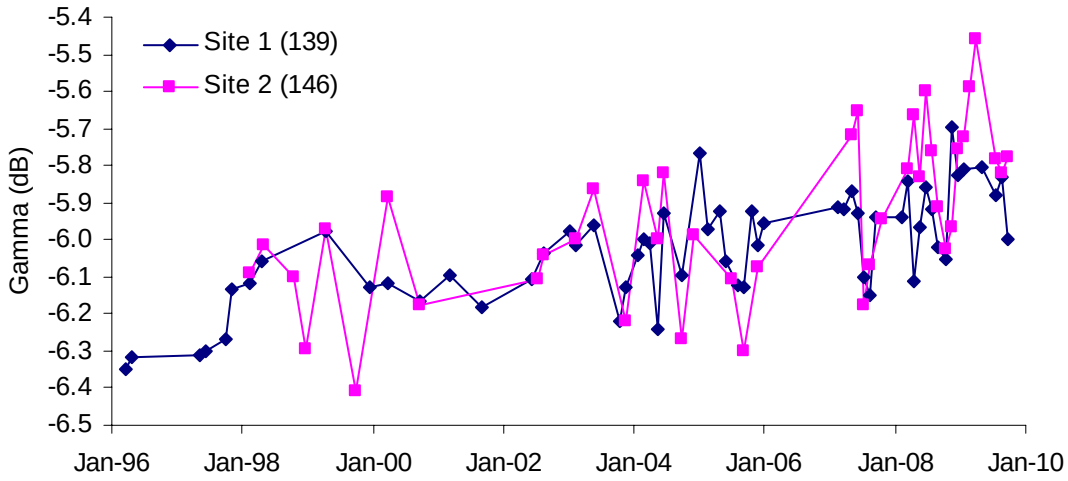

Figure 5.2. ERS-2 SAR Amazon Rainforest Stability

Ground stations can also be used to assess the stability of the ERS-2 SAR. As the ground station receiving dishes are acquiring and receiving data in real-time they will be pointing towards to satellite and hence appear as a point target in the SAR imagery. For the two 15m receiving dishes

at Kiruna, the point target response in processed imagery is so strong that it is saturated in the processed imagery. However, the azimuth ambiguities are not saturated and so have been used for stability assessment. At Neustrelitz there are three nearby 7.3m diameter receiving dishes which have a point target response that are not saturated in processed imagery and so can be used directly for stability assessment.

Table 5.3 gives the mean radar cross-section, stability and peak to peak radar cross-section values of the Kiruna ambiguities. These results are slightly higher than the transponder results given in Table 4.1. Figure 4.3 shows the ERS-2 Kiruna ambiguity radar cross-section for the two antennae (KS1 and KS2). For KS1 a change in the rcs measurements occurs at the same time as the start of gyro-less attitude control operation in early 2001. The measurement indicated by the red symbol has been corrected by 4dB due to the replica pulse problem that occurred from imagery acquired between 4th September and 14th October 2004. Since last 2006 the ERS-2 SAR products have been processed with the PGS-ERS processor rather than the VMP. It has been found that the azimuth ambiguity ratio from PGS-ERS images is about 3dB higher than from VMP images. In Figure 5.3 and Table 5.3 the PGS-ERS measurements have been corrected by 3dB (the dark blue measurements). All the KS2 measurements have been made using the PGS-ERS processor and include the 3dB correction. Hence the difference in rcs between KS1 and KS2 can be attributed to the receiving dishes themselves.

Note that the mean KS1 ambiguity radar cross-section derived using ERS-1 and ERS-2 imagery has been found to be similar indicating a good relative radiometric calibration between the two sensors.

Ground Station	Acquisition Dates	RCS (dBm^2)	Mean Stab. (dB)	P-P RCS (dB)	Num Results
KS 1	20-Jul-95 to 27-Jul-09	48.06	0.59	3.10	137
KS 2	18-Jan-07 to 19-Oct-09	43.15	0.48	2.51	48
NZ 1	13-Apr-96 to 29-Oct-09	58.93	0.54	3.39	139
NZ 2	15-Jan-98 to 07-Jun-09	59.36	0.52	2.96	90
NZ 3	09-Jan-03 to 13-Oct-09	63.59	0.32	1.78	53

Table 5.3. ERS-2 SAR radiometric results derived from the Kiruna (KS) and Neustrelitz (NZ) ground stations

Table 5.3 also gives the mean radar cross-section, stability and peak to peak radar cross-section values for the three Neustrelitz receiving dishes. Figure 5.4 shows the ERS-2 Neustrelitz ground station radar cross-sections. Although the three Neustrelitz ground stations are of the same diameter, the rcs of the newest antenna is significantly higher than the other two antennae. This is likely to be due to differences in the properties of each receiving dish. With the introduction of products from the PGS-ERS processor it was found that there was a jump in the measured rcs of the NZ3 receiving dish. This change was found to be due to the increase in the number of bits used in the detected product (from 15 to 16) which indicated that VMP measurements of this antennae were saturated (this was not the case of the NZ 1 and NZ 2 antennae). The radiometric stability and

peak to peak RCS results are slightly higher than for the ESA transponder. Examination of Figure 5.4 shows there are a small number of radar cross-section measurements that are significantly lower than the majority. Four of these occur when the ground station IRF is at extreme low and high incidence angles; it is suggested that the ground station itself is contributing to the larger than expected radar cross-section variations through mis-pointing and/or weather effects.

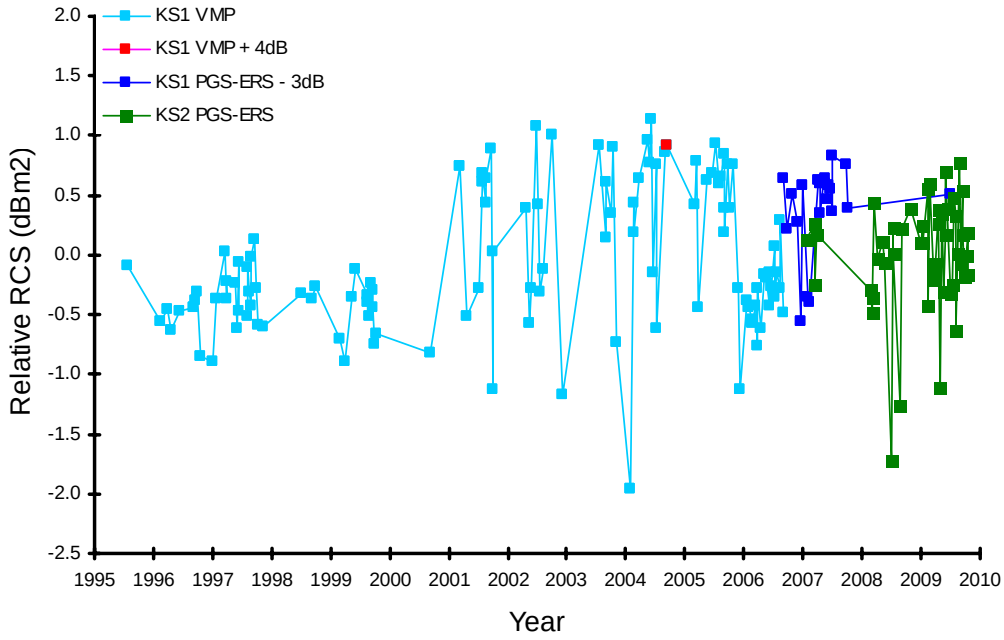

Figure 5.3. ERS-2 Kiruna ground station stability.

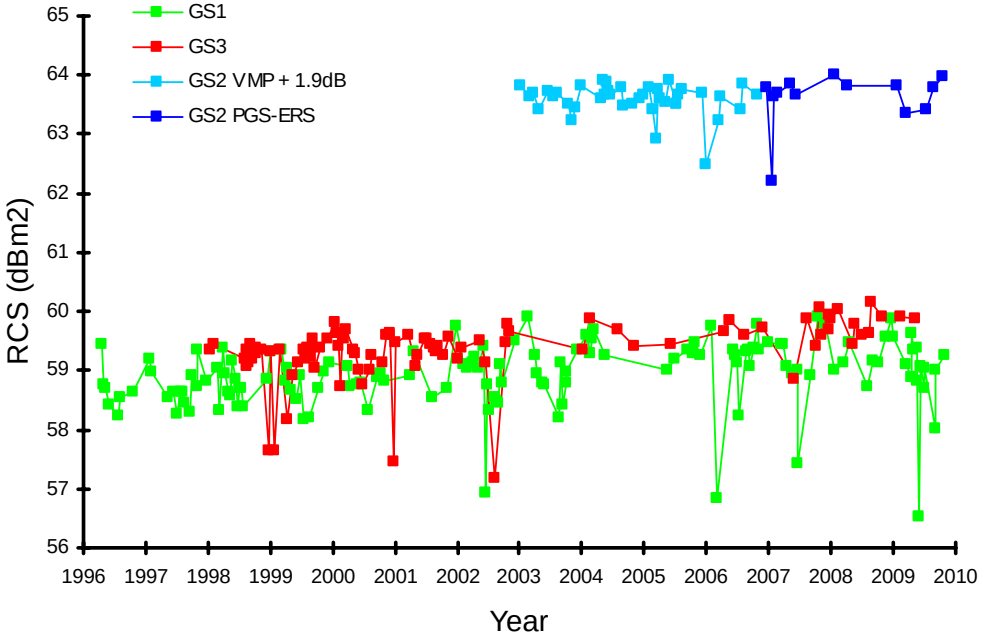

Figure 5.4. ERS-2 Neustrelitz ground station stability.

6 NOISE EQUIVALENT RADAR CROSS-SECTION

The upper limit to the noise equivalent σ^o ($NE\sigma^o$) of an image can be estimated by measuring the radar cross-section of low intensity regions (usually ocean/inland water regions). Figure 6.1 shows low intensity region radar cross-section measurements from PRI/IMP images (after removing the range dependence in $NE\sigma^0$ due to the elevation antenna pattern, range spreading loss and sin(i)/sin(23°) to give a $NE\sigma^0$ at the mid-swath position). The $NE\sigma^o$ measurements after the gain changes at the end of February 2003 are coloured red. $NE\sigma^0$ measurements extracted from imagery acquired between 4th September and 14th October 2004 have been reduced by 4dB to correct for the erroneous calibration attenuation gain setting during this period (coloured green). The brown data points are measurements made with PGS-ERS products. The trend line in Figure 6.1 is for (i) a 0.66dB per year decrease in transmitter pulse power between launch and the end of 2000, (ii) a decrease of 0.82dB per year until the end of February 2003, (iii) a 2dB drop at the end of February 2003 and then (iv) the resumption of the 0.66dB per year decrease.

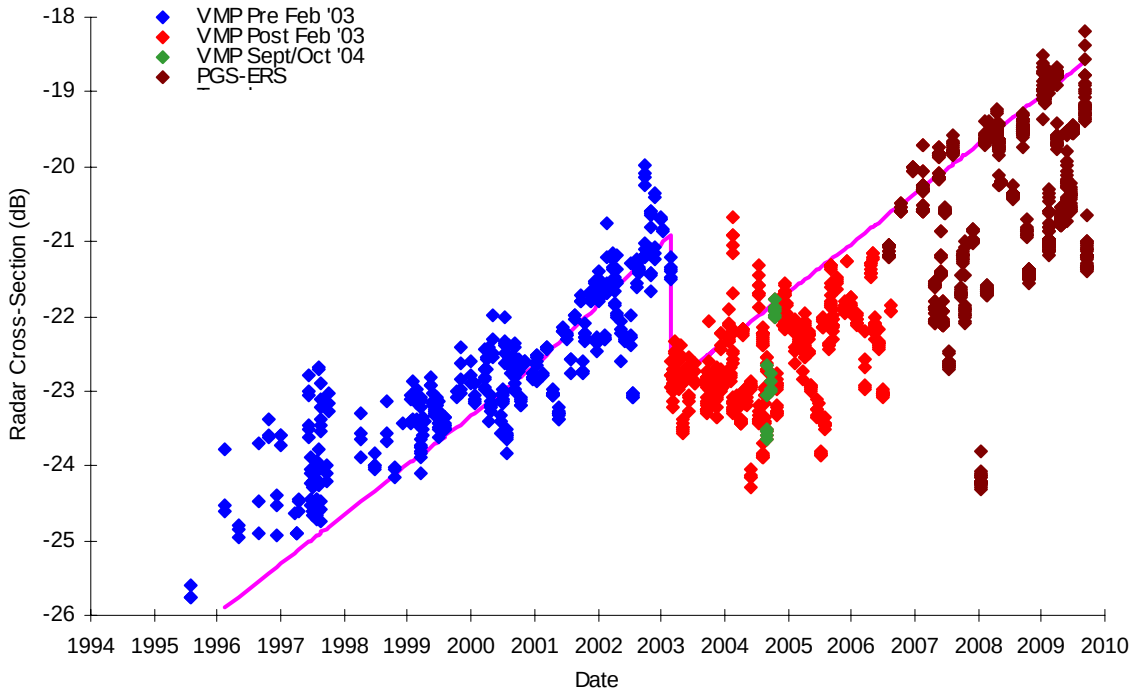

Figure 6.1. ERS-2 PRI/IMP estimate of Noise Equivalent Radar Cross-Section (at the mid-swath position) as a function of acquisition date.

An offset of 26.3dB has also been used for the trend line; -26.3dB represents the $NE\sigma^o$ at the start of the ERS-2 mission. Note that during mid-2000 and since mid-2001 there are $NE\sigma^0$ values below the trend line - this is due to imagery being used with higher replica and calibration pulse powers than the general downward trend in these powers. As the $NE\sigma^0$ is directly related to the

calibration and replica pulse powers, Figure 6.2 shows the NEσ^0 as a function of replica pulse power (the replica pulse power at the start of the mission has been set to 52.1dB). The lower trend line is a linear relationship between NEσ^0 and replica pulse power prior to the gain change at the end of February 2003 while the middle trend line is for this relationship after the gain change. Finally the upper trend line is for recent NESigma0 measurements from PGS-ERS products which are about 0.5dB higher than the post February 2003 VMP trend line. Figure 5.2 shows more clearly the reduction in NEσ^0 since the start of the ERS-2 mission.

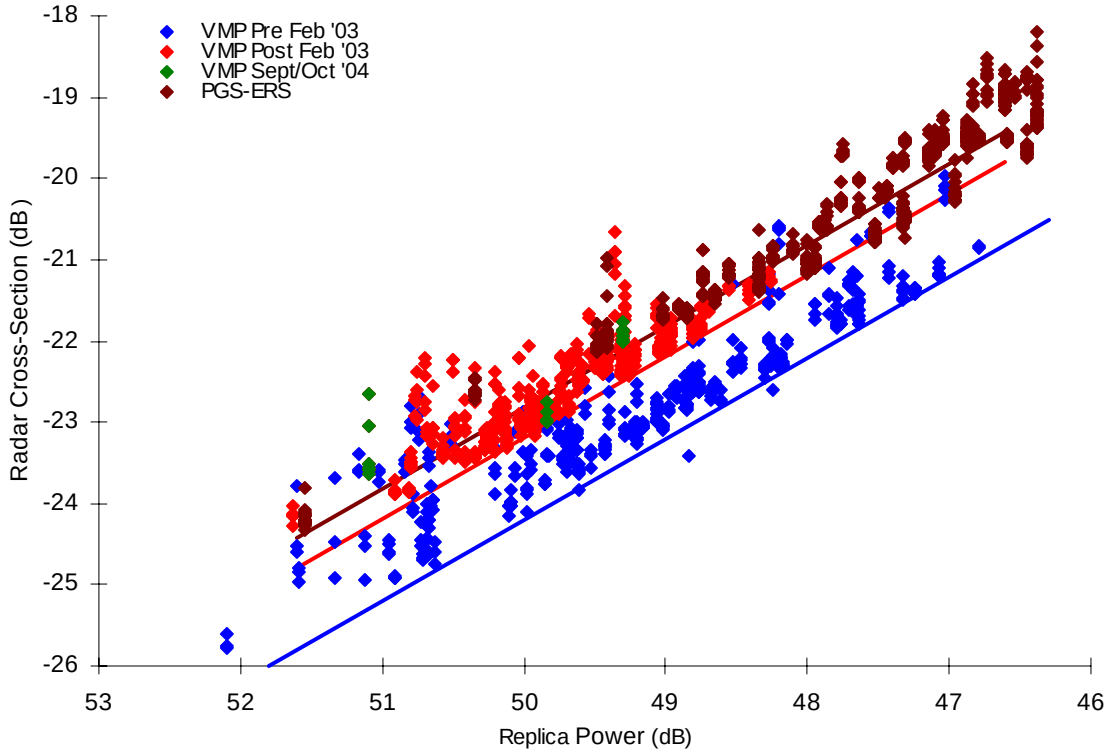

Figure 6.2. ERS-2 PRI/IMP estimate of Noise Equivalent Radar Cross-Section (at the mid-swath position) as a function of replica pulse power.

7 DOPPLER MONITORING

Figure 7.1 shows the Doppler centroid frequency and satellite yaw angle since the start the year 2000 when that attitude of the satellite was monitored by one gyroscope rather than 3 previously. Details of the evolution of the Doppler and yaw can be found in the ERS-2 SAR paper available on the ESA Product Control Service web site (http://earth.esa.int/pcs/ers/sar/articles/).

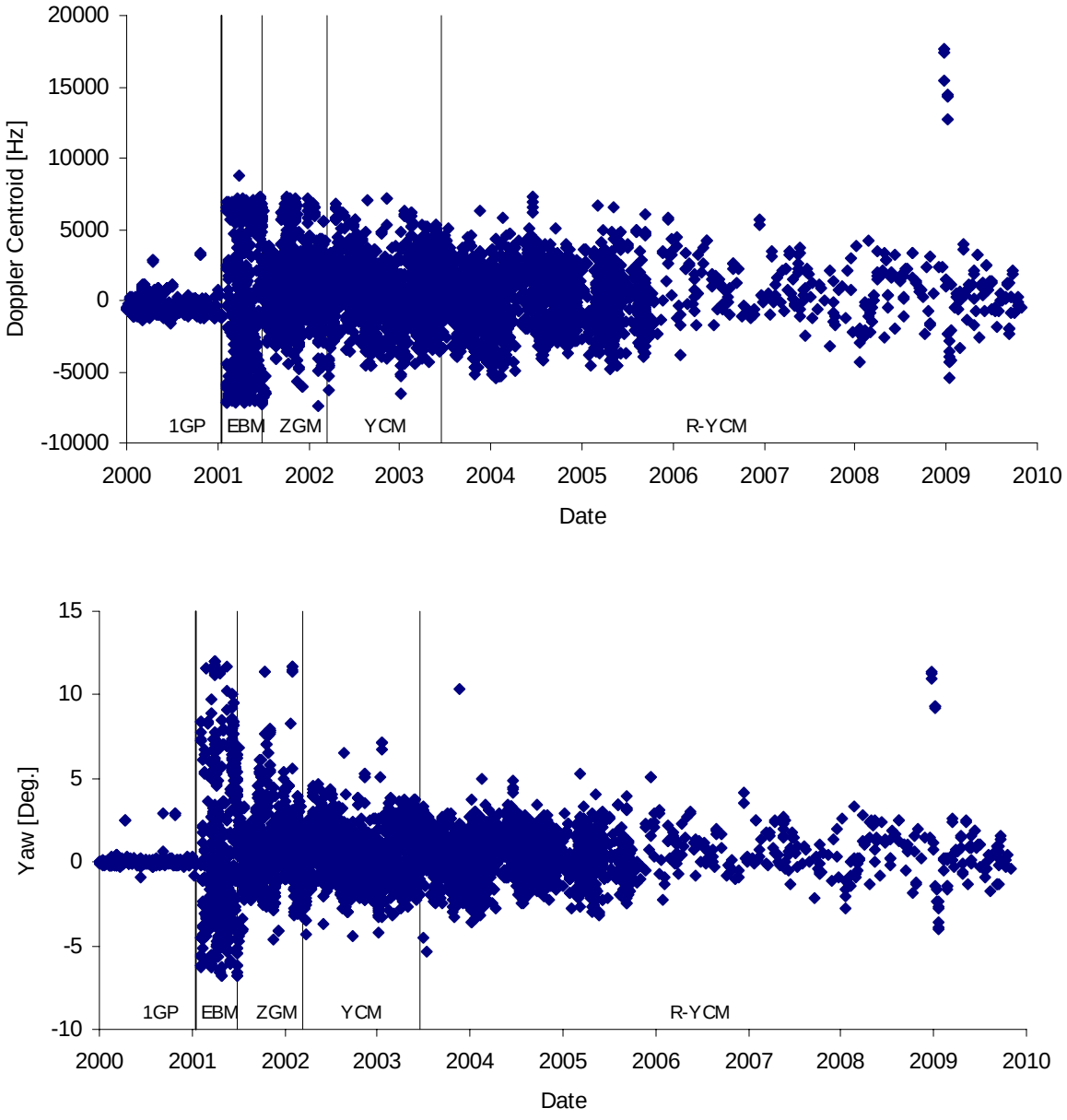

Figure 3.1. ERS-2 SAR Doppler Centroid (top) and Yaw (bottom) Evolution since January 2000

The very high Doppler and yaw values at the end of 2008/early 2009 were caused by a problem with the Digital Earth Sensor being occasionally being blinded by the Sun. Such blinding is autonomously detected on board and the spacecraft is left to drift until valid DES data is available again. This problem has also been identified during similar periods from previous years but not to the same extent.

ERS-2 Orbit Control Manoeuvres (OCM) can affect the platform attitude stability even hours after the burst with a direct impact on the Doppler centroid frequency evolution. An updated list of the OCM can be found at http://nng.esoc.esa.de/ers/ERSman.html.

8 AUXILIARY FILES

ERS-2 SAR auxiliary files contain information on calibration, the elevation antenna pattern and other instrument parameters. The files issued to date are:

ER2_XCA_AXNXXX20050321_000000_19950101_000000_20100101_000000
ER2_CON_AXNXXX20050321_000000_19950101_000000_20100101_000000

Note that the first date in the auxiliary files is the creation date, while the following dates indicate the start and stop of the file validity period. These files can be downloaded from http://earth.esa.int/pcs/ers/sar/aux/.